Korean J. Chem. Eng., 33(1), 90-98 (2016)
DOI: 10.1007/s11814-015-0096-9

pISSN: 0256-1115
eISSN: 1975-7220

Optimization of biodiesel production from a calcium methoxide catalyst using a statistical model

Warakom Suwanthai*, Vittaya Punsuvon*,,†, and Pilanee Vaithanomsat*****

*Department of Chemistry, Faculty of Science, Kasetsart University, Bangkok 10900, Thailand
**Center of Excellence-Oil Palm, Kasetsart University, Bangkok 10900, Thailand
***Kasetsart Agricultural and Agro-Industrial Product Improvement Institute, Kasetsart University, Bangkok 10900, Thailand
(*Received 10 November 2014 • accepted 12 May 2015*)

Abstract−Calcium methoxide catalyst was synthesized from quick lime and methanol, and further characterized using scanning electron microscopy (SEM), X-ray diffraction (XRD), attenuated total reflection Fourier transform infrared spectroscopy (ATR-FTIR), and energy dispersive X-ray spectroscopy (EDX). Response surface methodology (RSM) with a 5-level-3-factor central composite was applied for the calcium methoxide catalyzed transesterification of refined palm oil to investigate the effect of experimental factors on the methyl ester yield. A quadratic model with an analysis of variance (ANOVA) obtained from RSM is suggested for the prediction of methyl ester yield, and reveals that 95.99% of the observed variation is explained by the model. The optimum conditions obtained from RSM were 2.71 wt% of catalyst concentration, 11.5 : 1 methanol-to-oil molar ratio, and 175 min of reaction time. Under these conditions, the produced biodiesel met the standard requirements for methyl ester yield.

Keywords: Biodiesel, Calcium Methoxide, Transesterification, Response Surface Methodology, Refined Palm Oil

INTRODUCTION

As a consequence of the depletion of fossil resources, more attention has been redirected to the identification of environmentally friendly and renewable sources as alternatives to mineral oil. Vegetable oils are renewable raw materials and a promising feedstock for biodiesel production. At present, the majority of biodiesel is prepared by the transesterification of vegetable oils or animal fats using methanol or ethanol in the presence of a homogeneous catalyst, such as sodium hydroxide or potassium hydroxide. The homogeneous catalyst generates large volumes of waste water that must be treated, and significantly adds to the cost and environmental impact of the process [1]. Therefore, there has been renewed interest in the use of heterogeneous catalysts because they have many advantages, such as being noncorrosive, easier to separate, and economically and environmentally friendly. Triglyceride heterogeneous catalysts for transesterification reactions, such as alkali metal oxides, alkaline earth metal oxides, transition metal oxides, mixed metal oxides, and other derivatives, have been reported in the literature for a variety of applications, including ion exchange resins, sulfated oxide, waste materials, and enzymes [2].

Quick lime, or burnt lime, is calcium oxide (CaO) obtained by the calcination of pulverized limestone. Quick lime is a nontoxic material that is inexpensive, environmentally friendly, and commercially available in Thailand. The catalytic activity of quick lime can be increased by converting it to calcium methoxide ($Ca(OCH_3)_2$). Compared to CaO, this catalyst has higher activity and very low solubility in the transesterification reaction of vegetable oil [3]. In previous work, Liu et al. [4] synthesized $Ca(OCH_3)_2$ by a direct reaction between calcium metal and methanol at 65 °C for 4 h, and then used it as the catalyst in the transesterification reaction of soybean with methanol to produce biodiesel. Masood et al. [5] also synthesized $Ca(OCH_3)_2$ through a reaction between CaO and methanol under reflux conditions at 65 °C for 2 h. The obtained catalyst was used in the transesterification reaction between palm oil methyl ester and trimethylolporpane (TMP) to form a TMP triester product.

Refined palm oil (RBD) was obtained from a physical oil refinery plant. The oil passes through three refining steps (degumming, bleaching, and deodorizing) to remove impurities in the crude palm oil. RBD contains a low free fatty acid (FFA) content (around 0.1 wt%); thus, it is suitable for making biodiesel via transesterification without any problems caused by salt formation.

Response surface methodology (RSM) has been applied to analyze research involving a complex variable process. RSM employs multiple regression and correlation analyses to assess the effects of two or more independent factors on the dependent variables. Its principal advantage is in reducing the number of experimental runs required to generate sufficient information for a statistically acceptable result. RSM has been successfully applied in the study and optimization of biodiesel production from various feed stocks [6,7]. In addition, the central composite rotatable design (CCRD) of RSM has previously been applied in the optimization of several biotechnological and chemical processes [8].

In this study, $Ca(OCH_3)_2$ was prepared from quick lime and its physical and chemical properties were analyzed. The synthesized $Ca(OCH_3)_2$ was also tested as a solid catalyst in the transesterification of refined palm oil. RSM was utilized for process optimization, with the aim to better understand the relationships among

†To whom correspondence should be addressed.
E-mail: fscivit@ku.ac.th

three operating variables (methanol-to-oil molar ratio, catalyst concentration, and reaction time), as well as to improve upon the optimal conditions of a conventional experiment. The efficiency and reusability of $Ca(OCH_3)_2$ in biodiesel production were also studied.

EXPERIMENTAL

1. Materials

Quick lime and refined palm oil were kindly supplied by Panjapol Paper Industry Co., Ltd. (Saraburi, Thailand) and Patum Vegetable Oil Co., Ltd. (Pathum Thani, Thailand), respectively. Standard methyl heptadecanoate and standard chromatographic grade fatty acid methyl esters (FAME) were obtained from Fluka (Switzerland) and Sigma-Aldrich (Switzerland), respectively. Analytical grade methanol and n-heptane were purchased from Merck (Germany).

2. Characterization of Refined Palm Oil

A sample (40 mg) of RBD was placed in a 50 ml three-necked flask with a boiling chip, and 5 ml of 0.5 N methanolic sodium hydroxide was added to a sample flask connected to a condenser. The solution was refluxed at 90 °C until the fat globules disappeared (about 5 to 10 min). Then, 5 ml of boron trifluoride solution (BF_3, 14%v/v) was added through a condenser and boiling continued for 2 min, after which 5 ml of n-heptane was added followed by boiling for another 1 min. After the reaction was complete, the solution was cooled to room temperature, and 15 ml of saturated sodium chloride solution was added, followed immediately by 15 sec of shaking. The mixture was allowed to rest and separate into two layers. The upper layer of the solution was analyzed by gas chromatography (GC) to determine its fatty acid composition.

3. Preparation and Characterization of $Ca(OCH_3)_2$

Quick lime was ground manually using a mortar and pestle, and then passed through a 60-mesh screen to obtain a fine powder. The quick lime powder was further subjected to heat treatment in a furnace at 700 °C for 2 h. Subsequently, 5 g of the calcined quick lime powder was placed in a glass flask with 150 ml of methanol. The methanol was mixed with the quick lime powder at 65 °C and maintained at this temperature for 2 h while vigorously stirring. The residual $Ca(OCH_3)_2$ was collected by filtration and finally dried in an oven at 105 °C for 1 h. The synthesis reaction of $Ca(OCH_3)_2$ is shown in Eq. (1).

$$CaO + 2CH_3OH \rightarrow Ca(OCH_3)_2 + H_2O \quad (1)$$

The resultant $Ca(OCH_3)_2$ was characterized extensively. X-ray diffraction (XRD) patterns were recorded using a D8 Advance Bruker diffractometer (USA) with Cu K_α radiation. The analysis scanned a 2θ range from 5° to 40°. The surface functional groups of the $Ca(OCH_3)_2$ were determined by attenuated total reflection Fourier transform infrared spectroscopy (ATR-FTIR) on a Bruker Equinox 55 FTIR spectrometer (USA). The $Ca(OCH_3)_2$ powder was analyzed over a scanning range of 500-4,000 cm^{-1}. The textural and physical appearances were imaged using scanning electron microscopy (SEM) on a FEI Quanta 450 SEM (USA). Prior to imaging, the samples were covered with gold and mounted on a carbon film. The total surface area, total pore volume, and average pore diameter were determined by the BET (Brunauer-Emmett-Teller) method with a Quantachrome Autosorb 1 (USA). The chemical composition of the $Ca(OCH_3)_2$ was determined by energy-dispersive X-ray spectroscopy (EDX) on an X-Max^N Silicon drift detector (Oxford Instruments, High Wycombe, UK). The basic strengths (H_) were determined using Hammett indicators [9]. The indicators used were phenolphthalein (H_=9.3), 2, 4-dinitroaniline (H_=15.0), and 4-nitroaniline (H_=18.4).

4. Transesterification Process

The transesterification reactions were conducted in a laboratory-scale setup using a three-necked 100 ml flask equipped with a reflux condenser and a thermometer on a magnetic, heated stirrer set to 65°C and 750 rpm. The $Ca(OCH_3)_2$ was added to the flask when the reactants reached the required temperature. After the reaction was complete, the product was separated by centrifugation. The top layer consisted of biodiesel and the bottom layer contained a mixture of glycerol and $Ca(OCH_3)_2$. The excess methanol contained in the biodiesel was further removed in a rotary evaporator at 65°C. The obtained purified biodiesel was then bottled and stored for characterization.

5. Experimental Design and Statistical Analysis

Before RSM was performed, the relevant variables ($Ca(OCH_3)_2$ concentration, methanol-to-oil molar ratio and reaction time) for biodiesel production were selected by varying one factor at a time while holding the others constant. First, five different $Ca(OCH_3)_2$ concentrations (1-5 wt%) were examined, while the methanol-to-oil molar ratio and reaction time were held at 12 : 1 and 180 min, respectively. Then, the methanol-to-oil molar ratio was varied from 6 : 1 to 14 : 1 while holding the reaction time at 180 min. Finally, the reaction time was varied ranging from 60 to 300 min while using the optimal $Ca(OCH_3)_2$ concentration and methanol-to-oil molar ratio from the previous steps.

RSM with central composite design (CCD) was used to optimize the biodiesel production process and to investigate the influence of different process variables on the percentage of fatty acid methyl ester (%FAME). At five levels of independent variables ranging from −1.68 to +1.68, 20 experimental runs were carried out with the three independent variables: catalyst concentration, wt%, (A); methanol-to-oil molar ratio (B); and reaction time, h, (C). In addition, the 20 runs included 8 factorial points, 6 axial points, and 6 replicates at the center point to determine the experimental error in this study.

The experimental data were analyzed by using a second-order polynomial (Eq. (2)) to find the relationship between the independent variables and %FAME:

$$Y = \beta_0 + \sum_{i=1}^{3}\beta_i X_i + \sum_{i=1}^{3}\beta_{ii} X_i^2 + \sum_{i=1}^{2}\sum_{j=i+1}^{3}\beta_{ij} X_i X_j \quad (2)$$

where Y is the response (%FAME), β_0 is the intercept, β_i, β_{ii} and β_{ij} are the linear, quadratic, and interactive coefficients, respectively, and X_i and X_j are the independent variables. Statistical analysis of the equation was employed to evaluate the analysis of variance (ANOVA) and Design-Expert 8 software (State Ease Inc., Minneapolis, MN, USA) was used to design the experiments and carry out the regression and graphical analysis of the data.

6. Gas Chromatography (GC) Analysis

The FAME composition of the produced bio-diesel was analyzed by GC. The analysis was by a Chrompack CP9002 gas chromato-

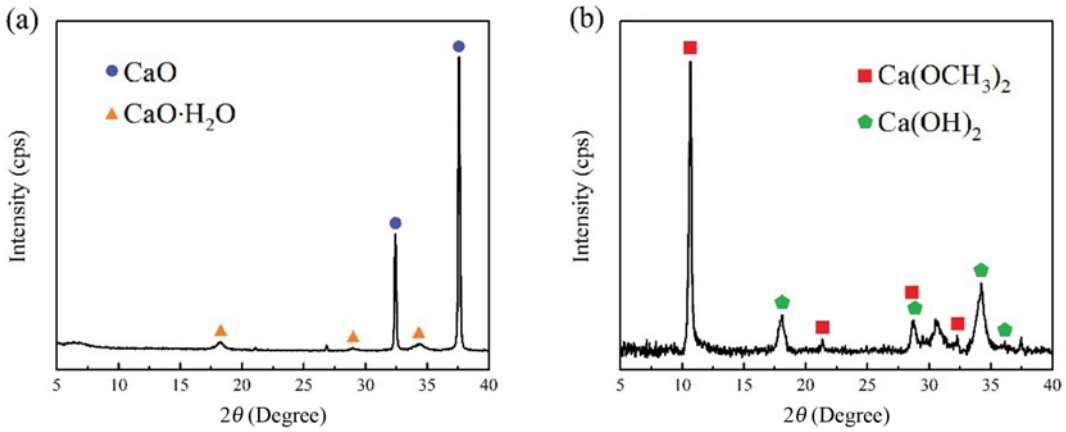

Fig. 1. XRD patterns of: (a) Calcined quick lime; (b) $Ca(OCH_3)_2$.

graph equipped with a DB-WAX capillary column (0.32 mm×30 m×0.25 μm film) and a flame ionization detector. Pure helium was used as a carrier gas (3 ml/min), with a 270 °C injector temperature, 300 °C detector temperature, split ratio of 1 : 30, sample size of 1 μl, and a temperature program of 80-250 °C at a fixed rate of 10 °C/min. The identification of FAME was established using a chromatographic reference mixture of standard FAME. The FAME content was calculated by taking the ratio of the total FAME peak areas to the peak area of the internal standard heptadecanoate (C_{17}).

7. Physical-chemical Characterization of Produced Biodiesel

The purified product obtained from transesterification was evaluated for its fuel properties following the recommended standard methods: kinematic viscosity at 40 °C (ASTM D445), density at 15 °C (EN ISO 3675), flash point (ASTM D93), acid value (ASTM D664), water and sediment (ASTM D2709), and methyl ester (EN 14103). All properties were analyzed in two replicates, and the data are reported as average values.

RESULTS AND DISCUSSION

1. Characterization of Refined Palm Oil (RBD)

The fatty acid profile of the RBD reveals that palmitic acid (42.83%) and oleic acid (39.59%) are the two major fatty acids, followed by linoleic acid (9.40%) and stearic acid (4.43%). The minor fatty acids are lignoceric acid (1.69%), myristic acid (0.94%), arachidic acid (0.35%), lauric acid (0.32%), behenic acid (0.16%), linolenic acid (0.15%) and palmitoleic acid (0.14%). The average molecular weight of RBD calculated from the fatty acid profile is 854.45 g/mol. The RBD also contains 0.1 wt% of FFA.

2. Characterization of $Ca(OCH_3)_2$

The crystal structure and symmetry of each sample were compared with the standard powder diffraction pattern in the database of the International Centre of Diffraction Data (ICDD). The calcium hydroxide $Ca(OH)_2$ and calcium carbonate ($CaCO_3$) impurities were removed from the quick lime by calcination at 700 °C for 2 h in a furnace. The XRD pattern indicates that calcination yields high purity CaO in the calcined quick lime, as shown in Fig. 1(a). The two diffraction peaks at 2θ of 32.41° and 37.6° are attributed to the CaO phase (ICDD file No. 00-001-1160) as a major component. The presence of calcium oxide hydrate ($CaO·H_2O$, ICDD file No. 00-002-0969) is also observed at 2θ of 18.12°, 28.77°, and 34.19°. The presence of $CaO·H_2O$ results from interactions between moisture and the surface of the CaO catalyst.

The calcined quick lime was further reacted with methanol under reflux conditions to transform the CaO into $Ca(OCH_3)_2$, and the diffraction pattern is shown in Fig. 1(b). The two peaks of CaO disappear while four peaks arise from $Ca(OCH_3)_2$ (ICDD file No. 00-031-1574) at 2θ of 10.65°, 21.36°, 28.41°, and 32.22°. This result is similar to those reported in previous research [5,9], which confirmed the presence of $Ca(OCH_3)_2$. However, four peaks at 2θ of 18.07°, 28.75°, 34.17°, and 36.61° are also indicative of $Ca(OH)_2$ (ICDD file No. 01-070-5492), which possibly appear due to interactions between CaO and water molecules during the synthesis reaction [5]. In addition, XRD analysis by DIFFRAC.EVA V2 software reveals the percentage yields of $Ca(OCH_3)_2$ and $Ca(OH)_2$ in the synthesized catalyst. The obtained percentage yields are 88.93% $Ca(OCH_3)_2$ and 11.07% $Ca(OH)_2$.

Fig. 2 shows the ATR-FTIR spectrum of the $Ca(OCH_3)_2$ product. The distinct peak at around 1,077 cm^{-1} (1) is assigned to the -C-O

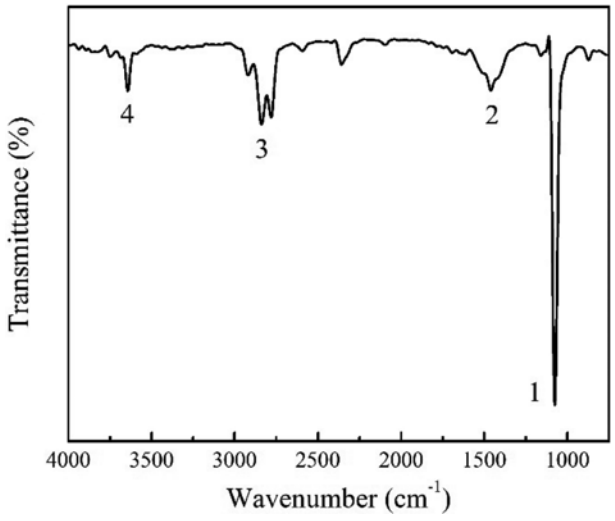

Fig. 2. ATR-FTIR spectrum of $Ca(OCH_3)_2$.

stretching vibration of primary alcohol. Another peak at around 3,650 cm^{-1} (4) is attributed to the -OH stretching vibration of primary alcohol. Other peaks at around 2,800-3,000 cm^{-1} (3) are derived from CH_3 stretching vibrations, and -C-H (alkane) bending is observed at 1,460 cm^{-1} (2) [4].

It was suggested previously that peak (4) arises from hydration on the surface of the $Ca(OCH_3)_2$. This peak indicates the existence of -OH groups isolated on the calcium cation that might have been produced interaction between water and the strongly basic $Ca(OCH_3)_2$ [5,10].

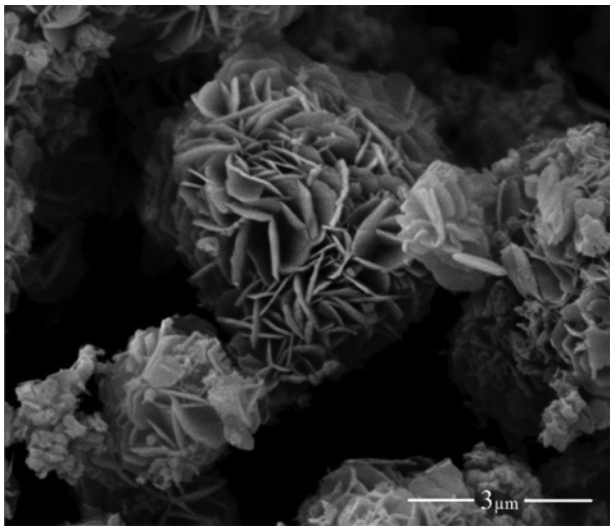

Fig. 3. SEM image of $Ca(OCH_3)_2$.

The shape and topology of the $Ca(OCH_3)_2$ particles are observed by SEM, as shown in Fig. 3. The morphology appears to be flower-like, consisting of thin plates. A large number of pores are visible on the surface. The BET surface area, total pore volume, and average pore diameter of the synthesized $Ca(OCH_3)_2$ were found to be 38.46 m^2g^{-1}, 0.33 cm^3g^{-1}, and 34.39 nm, respectively. High surface area and porosity are important characteristics of a solid catalyst since they are closely related to the catalytic activity [5]. To investigate the chemical composition of $Ca(OCH_3)_2$, EDX analysis was performed on a particular area of the $Ca(OCH_3)_2$ surface, and the at% calcium, oxygen, and carbon were determined to be 19.23%, 61.53%, and 19.24%, respectively. The calculated O:C atomic ratio from EDX was 3.2 : 1, which is higher than the theoretical ratio of 2 : 1 due to the adsorption of moisture on the surface of the catalyst. This result is supported by the FT-IR findings shown in Fig. 2.

The synthesized $Ca(OCH_3)_2$ changed the color of phenolphthalein (H_=9.3) from colorless to pink, and most of the $Ca(OCH_3)_2$ changed the color of 2,4-dinitroaniline (H_=15.0) from yellow to mauve. A few $Ca(OCH_3)_2$ samples failed to change the color of these indicators due to $Ca(OH_2)$ contamination while the color of 4-nitroaniline (H_=18.4) remained unchanged. Thus, the basic strength (H_) of $Ca(OCH_3)_2$ is between 9.3 and 18.4, and can be consid-

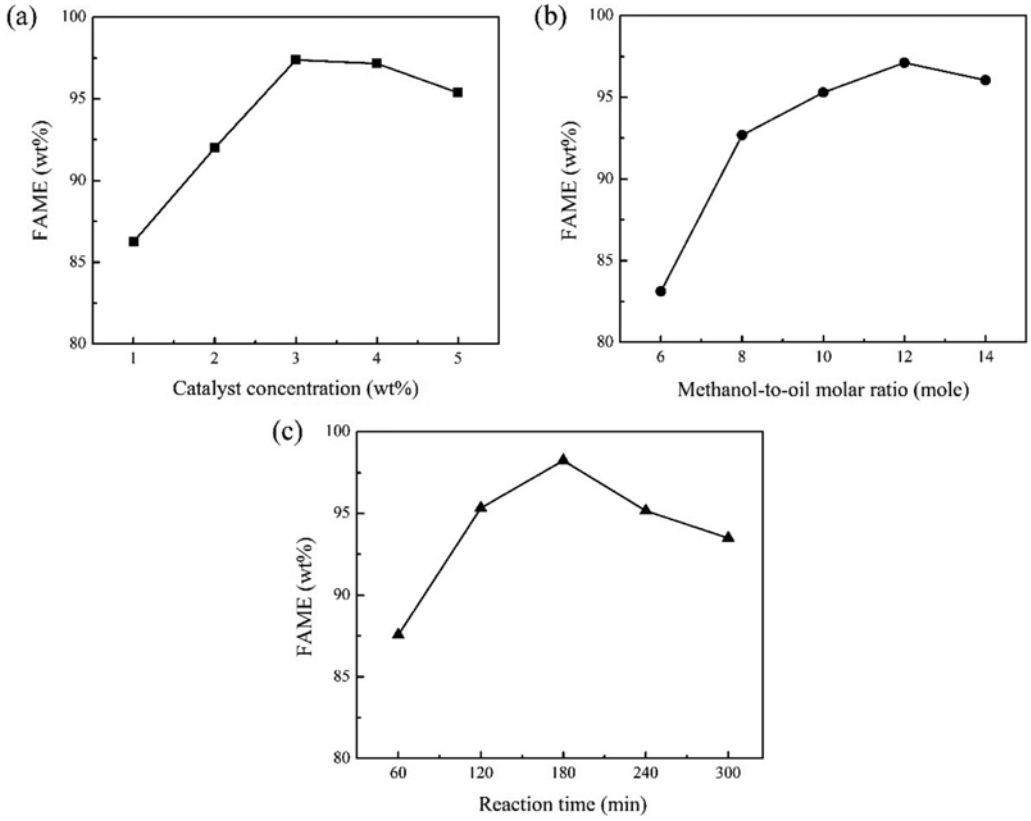

Fig. 4. FAME content in preliminary transesterifications as a function of: (a) Catalyst concentration; (b) methanol-to-oil molar ratio; (c) reaction time.

ered as a strong base for conducting transesterification [11].

3. Optimization of Reaction Conditions by RSM

Fig. 4(a)-(c) shows the preliminary transesterification conditions with 3 wt% catalyst, 12 : 1 methanol-to-oil molar ratio, and 180 min reaction time, which results in 97 wt% FAME. The obtained optimal conditions are further used in the CCD for RSM. The highest levels of FAME (wt%) from Fig. 4 are selected as the central point (0) values in CCD (2.5 wt% catalyst concentration, 8 : 1 methanol-to-oil molar ratio, and 120 min reaction time), as shown in Table 1.

In this research, the relationships between the response (%FAME) and the three reaction variables (catalyst concentration, methanol-to-oil molar ratio, and reaction time) were evaluated using RSM. The results at each point based on the experimental CCD are presented in Table 2. Twenty experiments were performed in duplicate.

Regression analysis was employed to fit the empirical model with the generated response variable data [12]. The response obtained in Table 2 was correlated with the three independent variables using a polynomial equation (Eq. (2)). The observed and predicted values of %FAME obtained at the design points of different reaction conditions are shown in Table 2. The %FAME varies between 37.16% and 97.37%. The minimum %FAME (37.16%) was obtained at 2.50% catalyst concentration, 10 : 1 methanol-to-oil molar ratio, and 19.09 min reaction time, while the maximum (97.37%) was produced at 3.50% catalyst concentration, 12 : 1 methanol-to-oil molar ratio, and 180 min reaction time.

Design-Expert 8 software was employed to determine and evaluate the coefficients of the full regression model equation and their statistical significance. The second polynomial model for the %FAME was regressed, as shown in Eq. (3):

$$Y=-58.640+20.981A+6.759B+0.930C-0.973AB -0.060AC-0.002BC+0.178A^2-0.123B^2-0.00244C^2 \quad (3)$$

where Y is the response variable of %FAME, and A, B, and C are the actual values of the predicted catalyst concentration, methanol-to-oil molar ratio, and time, respectively.

The obtained data were then analyzed using ANOVA for fitting a second-order response surface model by the least squares method and to assess the quality of the fit. The terms of the significant quadratic model for all responses are shown in Table 3. At the 95% confidence level, F_{model}=26.60 with a very low probability value ($p<0.05$) that the null hypothesis is correct, indicating the high significance of the fitted model and showing the reliability of the regression model for predicting the %FAME [13]. In addition, the factors of A, B, C, AC and C^2 were found to be significant at the 95% confidence level according to the computed *F*-values (high) and the *p*-value at the 5% level. These statistical tests indicate that the selected model is satisfactory for predicting the %FAME within the scope of the studied variables, and also shows that the quadratic model is valid in the present study. The smaller the *p*-value for a parameter, the more significant the parameter is [14].

The statistical significance of the fitted model parameters in Table

Table 1. Reaction condition variables and levels for CCD

Reaction condition variables	Symbol coded	Range and levels				
		−1.68	−1	0	+1	+1.68
Catalyst concentration (wt%)	A	0.82	1.5	2.5	3.5	4.18
Methanol-to-oil molar ratio	B	6.64	8	10	12	13.36
Reaction time (min)	C	19.09	60	120	180	220.91

Table 2. Experimental design with observed and predicted values from transesterification of refined palm oil

Run number	Catalyst concentration (wt%)	Methanol-to-oil molar ratio	Reaction time (min)	Observed FAME (%)	Predicted FAME (%)
1	1.50 (−1)	8.00 (−1)	60.00 (−1)	48.39	49.74
2	3.50 (+1)	8.00 (−1)	60.00 (−1)	73.67	70.73
3	1.50 (−1)	12.00 (+1)	60.00 (−1)	61.36	60.73
4	3.50 (+1)	12.00 (+1)	60.00 (−1)	75.40	73.95
5	1.50 (−1)	8.00 (−1)	180.00 (+1)	85.54	87.82
6	3.50 (+1)	8.00 (−1)	180.00 (+1)	92.98	94.44
7	1.50 (−1)	12.00 (+1)	180.00 (+1)	94.25	98.02
8	3.50 (+1)	12.00 (+1)	180.00 (+1)	97.37	96.86
9	0.82 (−1.68)	10.00 (0)	120.00 (0)	82.78	79.15
10	4.18 (+1.68)	10.00 (0)	120.00 (0)	93.37	95.82
11	2.50 (0)	6.64 (−1.68)	120.00 (0)	80.83	79.95
12	2.50 (0)	13.36 (+1.68)	120.00 (0)	91.54	91.24
13	2.50 (0)	10.00 (0)	19.09 (−1.68)	37.16	39.74
14	2.50 (0)	10.00 (0)	220.90 (+1.68)	94.80	91.04
15	2.50 (0)	10.00 (0)	120.00 (0)	85.24	86.98
16	2.50 (0)	10.00 (0)	120.00 (0)	92.96	86.98
17	2.50 (0)	10.00 (0)	120.00 (0)	79.79	86.98
18	2.50 (0)	10.00 (0)	120.00 (0)	84.25	86.98
19	2.50 (0)	10.00 (0)	120.00 (0)	88.05	86.98
20	2.50 (0)	10.00 (0)	120.00 (0)	91.40	86.98

Table 3. ANOVA for the response surface quadratic model

Source of variation	Sum of squares	df[a]	Mean square	*F*-value	*P*-value[b]	Significant at 5% level
Model	4651.99	9	516.89	26.60	<0.0001	Yes
A	335.51	1	335.51	17.27	0.0020	Yes
B	153.68	1	153.68	7.91	0.0184	Yes
C	3175.81	1	3175.81	163.44	<0.0001	Yes
AB	30.26	1	30.26	1.56	0.2405	No
AC	103.39	1	103.39	5.32	0.0438	Yes
BC	0.32	1	0.32	0.016	0.9004	No
A^2	0.46	1	0.46	0.024	0.8811	No
B^2	3.46	1	3.46	0.18	0.6819	No
C^2	839.77	1	839.77	43.22	<0.0001	Yes
Residual	194.31	10	19.43			
Lack of Fit	75.70	5	15.14	0.64	0.6829	No
Pure Error	118.61	5	23.72			
Total	4846.31	19				

[a]df is degree of freedom
[b]p>0.05 is not significantly different at the 5% level

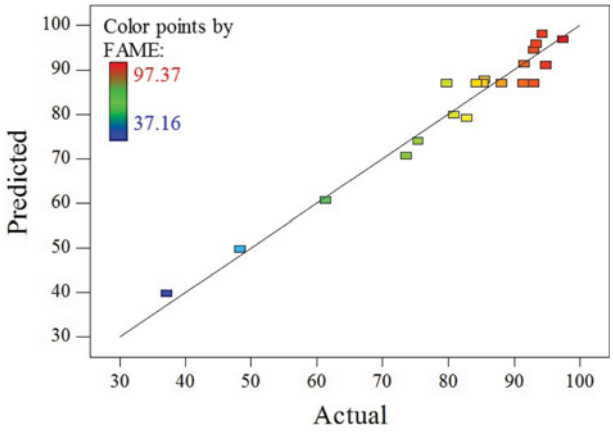

Fig. 5. Predicted %FAME versus actual %FAME plot.

3 reveals that reaction time has a large effect on the %FAME due to the high *F*-value and its corresponding low *p*-value. The *p*-value of the lack of fit was 0.6829, indicating that it was not significant. Therefore, the number of experiments was sufficient to determine the effect of the variables on %FAME [15]. The suitability of the model was also tested using the regression equation (Eq. (3)) and determination coefficient (R^2). The high value of R^2 (0.9599) indicates that the fitted model can be used to predict reasonably precise outcomes [16].

Fig. 5 shows that the response predicted from the empirical model is in agreement with the observed values in the range of the experimental variables. The value of the adjusted determination coefficient (R_{adj}^2=0.9238) is high, signifying the high significance of the model. A high value of the determination coefficient (R^2=0.9599) justifies the excellent correlation between the independent variables. On the other hand, a relatively low value of the coefficient of variation (CV=5.40%) reveals better precision and reliability for this fitted model [17].

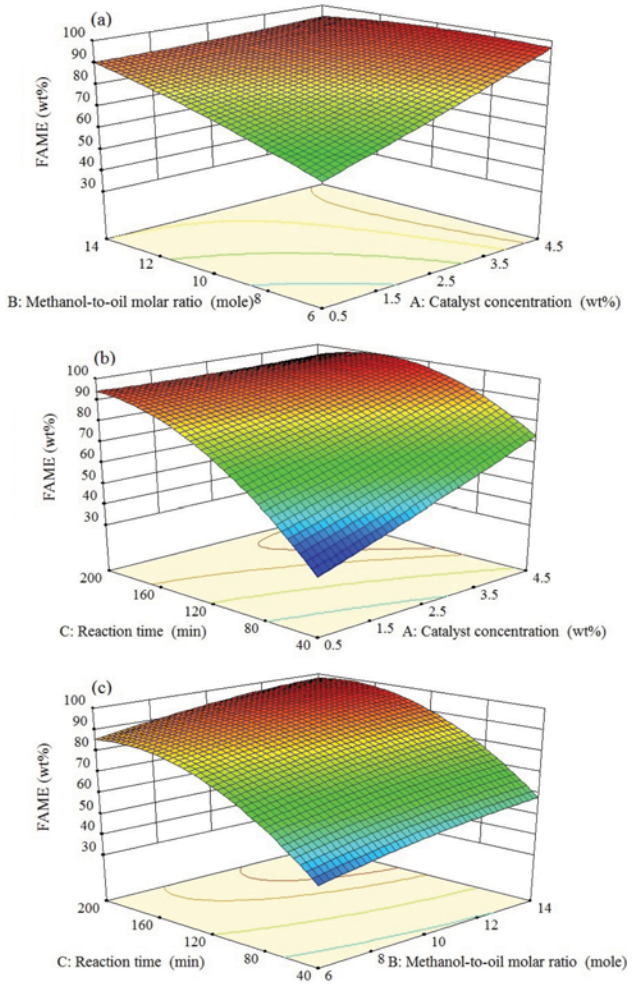

Fig. 6. Response surface plots elucidating the effects of (a) methanol-to-oil molar ratio and catalyst concentration; (b) reaction time and catalyst concentration; and (c) reaction time and methanol-to-oil molar ratio.

The response surface plot of %FAME from various combinations of catalyst concentration, methanol-to-oil molar ratio, and reaction time is shown in Fig. 6 and represents the graphical three-dimensional surface plot of Eq. (3).

Fig. 6(a) demonstrates the effect of varying the methanol-to-oil molar ratio and the catalyst concentration on the %FAME at a fixed reaction time (120 min). It is clear that an increase in %FAME occurs with increasing catalyst concentration and methanol-to-oil molar ratio. In general, the amount of heterogeneous catalyst has a significant positive effect on the transesterification of vegetable oil to methyl ester due to the number of active sites available for the reaction [18]. The high concentration of methanol promotes the reversible reaction in the forward direction resulting in a better %FAME [19].

Fig. 6(b) shows the effect of reaction time and catalyst concentration at a constant methanol-to-oil molar ratio (10 : 1). The results reveal an increased %FAME with increasing catalyst concentration. The %FAME also increases with increasing reaction time up to a maximum, after which further increases in reaction time lead to slight decreases in %FAME.

Fig. 6(c) shows the effect of reaction time and methanol-to-oil molar ratio on %FAME at a constant catalyst concentration (2.5 wt%). The %FAME increases with increasing methanol-to-oil molar ratio. The %FAME also increases with increasing reaction time, but again the %FAME slightly decreases at very high reaction times. This could be explained by the transesterification reaction between the oil and alcohol being reversible when the reaction time is too long [20].

The optimal transesterification conditions were predicted by applying numerical optimization with the Design Expert software using RSM, as shown in Table 4. The optimization criteria were set for both variables: the independent and the response. The goal of the response optimization was to maximize the %FAME. The lower limit of FAME content was set at 96.5% (European standard). The optimal conditions for producing the maximum %FAME (96.70%) are 2.71 wt% of catalyst, an 11.5 : 1 methanol-to-oil molar ratio, and 175 min of reaction time.

Experiments were also conducted to verify the accuracy of the predicted model. The optimal conditions were adopted thrice to confirm the experimental (observed) results as shown in Table 5. The predicted value of 96.70% was approximately equal to the observed average value of 98.16%. Therefore, the experimental values were in acceptable agreement with the predicted values, and the errors between the two values were small (<5% error for the %FAME). Table 5 shows a slight difference between the observed and predicted values of the %FAME. When the observed and predicted results are close, they represent a more adequate regression model.

Table 4. Numerical optimization of the reaction conditions using RSM

Solution no.	A	B	C	%FAME	Desirability	
1	2.71	11.50	174.97	96.70	0.979	Selected
2	2.65	11.50	174.99	96.69	0.978	
3	2.52	11.50	175.00	96.65	0.978	
4	2.51	11.50	174.99	96.65	0.978	
5	2.35	11.50	174.99	96.65	0.977	

4. Properties of Produced Biodiesel

The values of various properties were tested following the biodiesel standards of the USA (ASTM) and Europe (EN), as exhibited in Table 6. The results show that all biodiesel properties meet the standards.

5. Reusability of the Catalyst

Recycling the catalyst is an important step in minimizing the process cost. After the reaction, the catalyst was tested for its reusability. It was separated from the reaction mixture by centrifugation followed by washing with methanol and hexane to remove any adsorbed stains. Finally, the recovered catalyst was dried overnight at 105 °C in an oven.

The dried catalyst was then reused under optimal transesterification conditions (Fig. 7(a)) and under conditions with excess methanol (Fig. 7(b)). Fig. 7(a) shows that the catalyst could be reused up to three times while maintaining >84.74%FAME under optimal conditions. Interestingly, excess methanol in the transesterifi-

Table 5. Optimum reaction conditions and validation test

Exp. no.	A	B	C	Observed FAME (%)	Predicted FAME (%)	Error
	Optimal	Reaction	Conditions			
1	2.71	11.50	175	98.80	96.70	2.12
2	2.71	11.50	175	98.10	96.70	1.43
3	2.71	11.50	175	97.58	96.70	0.90

Table 6. Properties of RPO biodiesel

Parameter	Testing method	Specification	Biodiesel in this study
Viscosity at 40 °C (cSt)	ASTM D445	1.9-6.0	5.64
Density at 15 °C (g/cm^3)	EN ISO 3675	0.86-0.90	0.872
Flash point (°C)	ASTM D93	130 min.	166
Acid value (mg KOH/g)	ASTM D664	0.80 max.	0.27
Water and sediment (% v)	ASTM D2709	0.050 max.	0.04
Methyl ester (wt%)	EN 14103	≥96.5	98.34

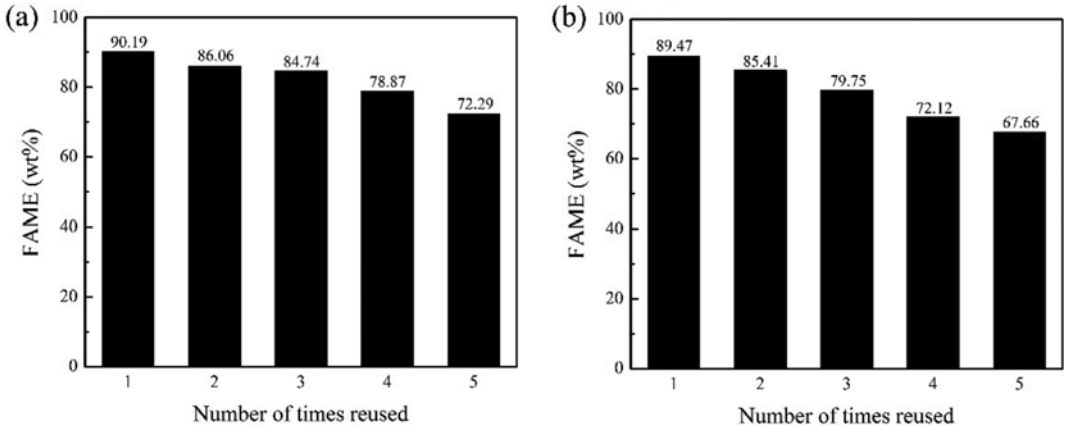

Fig. 7. Catalyst reusability testing from (a) optimal transesterification conditions (2.71 wt% catalyst, 11.5 : 1 methanol-to-oil molar ratio, and 175 min reaction time); (b) excess methanol transesterification conditions (2.71 wt% catalyst, 15 : 1 methanol-to-oil molar ratio, and 175 min reaction time).

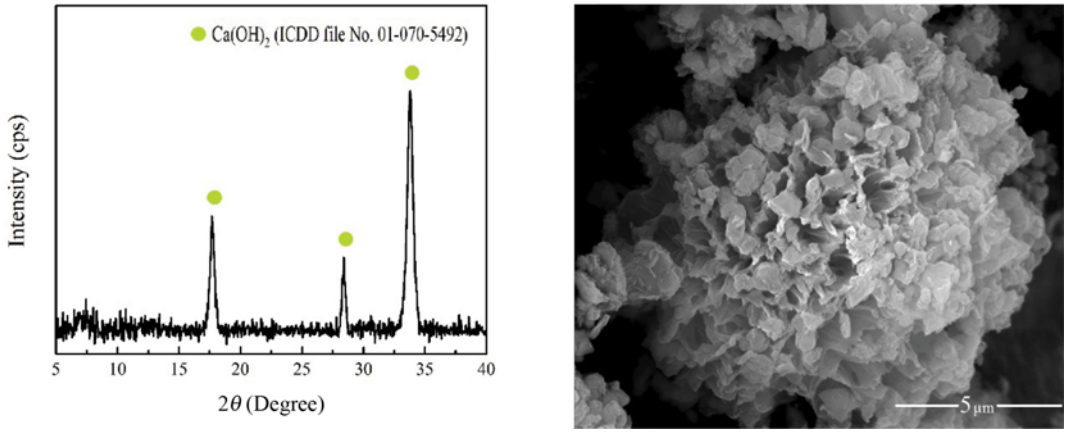

Fig. 8. XRD pattern and SEM image of reused $Ca(OCH_3)_2$ catalyst.

cation does not improve the reusability of the catalyst, as shown in Fig. 7(b). The deactivation of the recycled catalyst was found to result from changes in the catalyst surface by XRD and SEM imaging (Fig. 8). The XRD result reveals the disappearance of $Ca(OCH_3)_2$ and the introduction of $Ca(OH)_2$ on the catalyst surfaces.

CONCLUSION

RSM was applied to the transesterification reaction between RBD and methanol by using a laboratory-synthesized $Ca(OCH_3)_2$ catalyst. The significant merit of this technique is the short reaction time, small amount of catalyst, and low value of the methanol-to-oil molar ratio compared to conventional methods. The synthesized $Ca(OCH_3)_2$ provides high catalytic activity for transesterification in terms of FAME yield and reusability. These results suggest that $Ca(OCH_3)_2$ is a potential solid catalyst suitable for use in RBD biodiesel production.

ACKNOWLEDGEMENT

This work was supported by the Kasetsart University Research and Development Institute (KURDI).

NOMENCLATURE TABLE

A : predicted catalyst concentration [wt%]
B : predicted methanol-to-oil molar ratio [-]
C : predicted reaction time [h]
CV : coefficient of variation [%]
df : degrees of freedom [-]
%FAME : wt% fatty acid methyl esters [wt%]
F : *F*-factor [-]
p : probability value [-]
R^2 : determination coefficient [-]
R_{adj}^2 : adjusted determination coefficient [-]
X_i : independent variable (Eq. (2)) [-]
X_j : independent variable (Eq. (2)) [-]
Y : response (equivalent to %FAME) [-]
β_0 : intercept of Eq. (2) [-]
β_i : linear coefficient of Eq. (2) [-]
β_{ii} : quadratic coefficient of Eq. (2) [-]
β_{ij} : interactive coefficient of Eq. (2) [-]

REFERENCES

1. J. R. Kastner, J. Miller, D. P. Geller, J. Locklin, L. H. Keith and T. Johnson, *Catal. Today*, **190**, 122 (2012).
2. M. K. Lam, K. T. Lee and A. R. Mohamed, *Biotechnol. Adv.*, **28**, 500 (2010).
3. S. Gryglewicz, *Bioresour. Technol.*, **70**, 249 (1999).
4. X. Liu, X. Piao, Y. Wang, S. Zhu and H. He, *Fuel*, **87**, 1076 (2008).
5. H. Masood, R. Yunus, T. S. Y. Choong, U. Rashid and Y. Taufiq Yap, *Appl. Catal. A.*, **425-426**, 184 (2012).
6. J.-Y. Park, J.-S. Lee, Z.-M. Wang and D.-K. Kim, *Korean J. Chem. Eng.*, **27**(6), 1791 (2010).
7. W. Malilas, S. W. Kang, S. B. Kim, H. Y. Yoo, W. Chulalaksananukul and S. W. Kim, *Korean J. Chem. Eng.*, **30**(2), 405 (2013).
8. B. S. Gandhi and D. S. Kumaran, *Int. J. Green Energy*, **11**, 1084 (2014).
9. A. Kawashima, K. Matsubara and K. Honda, *Bioresour. Technol.*, **100**, 696 (2009).
10. H. D. Lutz, H. Müller and M. Schmidt, *J. Mol. Struct.*, **328**, 121 (1994).
11. P. L. Boey, G. P. Maniam, S. A. Amid and D. M. H. Ali, *Fuel*, **90**, 2353 (2011).
12. R. L. Mason, R. F. Gunst and J. L. Hess, *Statistical design and analysis of experiments: With applications to engineering and science*, John Wiley and Sons, New York (1989).
13. K. T. Lee, A. M. Mohtar, N. F. Zainudin, S. Bhatia and A. R. Mohamed, *Fuel*, **84**, 143 (2005).
14. A. I. Khuri and J. A. Cornell, *Response Surfaces: Designs and Analyses*, Marcel Dekker, New York (1987).
15. D. C. Montgomery, *Design and Analysis of Experiments 5th Ed.*, Wiley, New York (2001).
16. G. A. F. Seber, *Linear Regression Analysis*, John Wiley and Sons, New York (1977).
17. X. Yuan, J. Liu, G. Zeng, J. Shi, J. Tong and G. Huang, *Renew. Energy*, **33**, 1678 (2008).
18. G. Arzamendi, I. Campo, E. Arguiñarena, M. Sánchez, M. Montes and L. M. Gandía, *Chem. Eng. J.*, **134**, 123 (2007).
19. Z. Wan and B. H. Hameed, *Bioresour. Technol.*, **102**, 2659 (2011).
20. C. Samart, P. Sreetongkittikul and C. Sookman, *Fuel Process. Technol.*, **90**, 922 (2009).